UNIVERSITAT AUTÒNOMA DE BARCELONA

DEPARTAMENT DE GEOLOGIA
UNITAT DE CRISTAL·LOGRAFIA I MINERALOGIA

Caracterización y origen de los depósitos de Zn-(Fe-Pb) en la zona de Riópar (Prebético, SE de España)

TESIS DOCTORAL

DÍDAC NAVARRO CIURANA

SETIEMBRE DE 2016

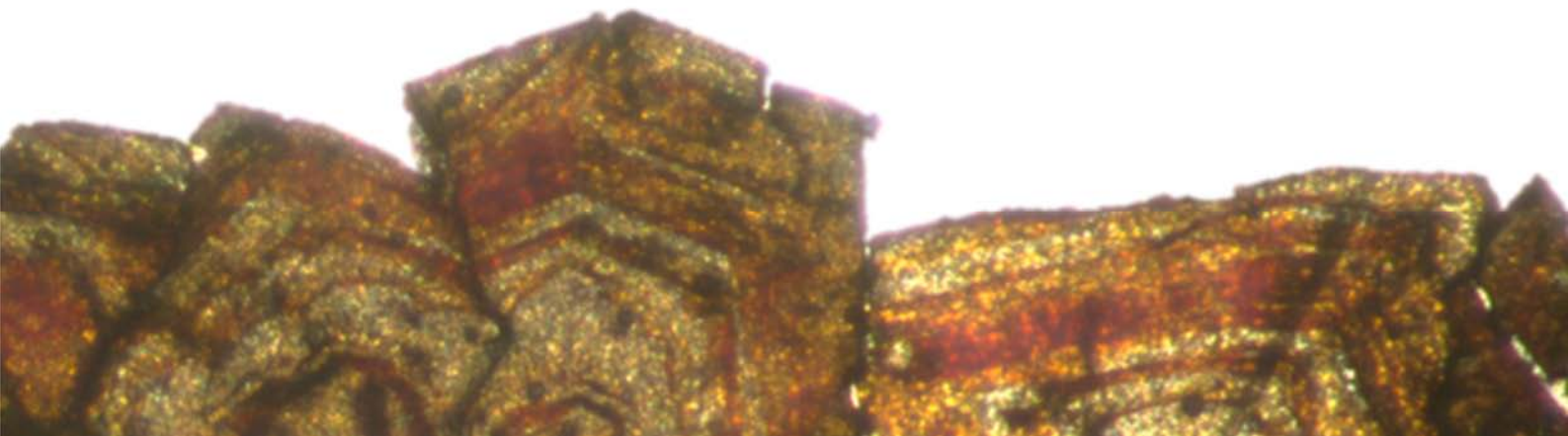

Anexos

Anexo 1. Navarro-Ciurana, D., Griera, A., Gómez-Gras, D., Cardellach, E., Vindel, E., Corbella, M. (2016): Dolostone origin in the Riópar area (SE Spain): implications on the geology of the Prebetic Zone. Resumen Extenso presentado en el *IX Congreso Geológico de España*, Huelva, España;

Anexo 2. Navarro-Ciurana, D., Corbella, M., Gómez-Gras, D., Griera, A., Vindel, E., Cardellach, E., (2015): Relationship between dolomite textures and formation temperature – insights from the Riópar Area (Betic basin, SE Spain). Resumen Extenso Tu N110 07, presentado en el *77th European Association of Geoscientists and Engineers Conference Exhib*., Madrid, España. http://dx.doi.org/ 10.3997/2214-4609.201412661;

Anexo 3. Navarro-Ciurana, D., Cardellach, E., Galindo, C., Fuenlabrada, J.M., Griera, A., Gómez-Gras, D., Vindel, E., Corbella, M. (2016): REE and Sm-Nd clues of high-temperature fluid-rock interaction in the Riópar dolomitization (SE Spain). Aceptado a *Procedia Earth and Planetary Science*. Resumen Extenso presentado en el *15th Water-Rock Interaction International Symposium*, WRI-15, Évora, Portugal;

Anexo 4. Navarro-Ciurana, D., Corbella, M., Griera, A., Gómez-Gras, D., Vindel, E., Daniele, L., Cardellach, E., (2015): Geochemical evidences and heat-transport simulations for warm fluid involvement in the formation of Riópar MVT deposit (Prebetic Basin, SE Spain). Resumen Extenso S3-P18, presentado en la *Society for Geology Applied to Mineral Deposits 13th Biennial Meeting*, Nancy, Francia.

ANEXO

1

Origen de las dolomías en la zona de Riópar (SE de España): implicaciones sobra la geología de la Zona Prebética

Dolostone origin in the Riópar area (SE Spain): implications on the geology of the Prebetic Zone

Origen de las dolomías en la zona de Riópar (SE España): implicaciones sobre la geología de la Zona Prebética

D. Navarro-Ciurana[1], A. Griera[1], D. Gómez[1], E. Cardellach[1], E. Vindel[2] and M. Corbella[1]

1 Departament de Geologia, Facultat de Ciències, Universitat Autònoma de Barcelona, Edifici Cs s/n, 08193 Bellaterra, Cerdanyola del Vallès, España.
2 Departamento de Cristalografía y Mineralogía, Facultad de Ciencias Geológicas, Universidad Complutense de Madrid, c/ José Antonio Novais s/n, 28040, Madrid, España.

Abstract: In the present study a petrographic description and C-O stable isotope data of dolostone occurrences at the Riópar area (Mesozoic Prebetic Zone) are presented. Results constrain the origin and dolomitization processes for each dolomitic unit providing new insights on the geology of the Prebetic. Dolostones are grouped in: i) large seismic-scale stratabound dolostones hosted in limestones of Lower Jurassic, Middle Jurassic and Upper Cretaceous ages; and ii) stratabound and patchy dolostones hosted in a carbonatic sequence of Upper Jurassic to Lower Cretaceous age. Two dolomitizing origins have been distinguished: i) a low-temperature dolomitization originated from seawater (seismic-scale stratabound dolomitized limestones); ii) a hydrothermal dolomitization originated by high temperature brines (stratabound and patchy dolomitized limestones). Results of this study can be used as a guide for other poorly known dolomitic areas in the Prebetic Zone.

Key words: dolostone, stable isotope, Prebetic, Riópar.

Resumen: *En este estudio se presenta la descripción petrográfica y los datos isotópicos de C y O de distintos cuerpos de dolomías en la zona de Riópar (Zona Mesozoica del Prebético). Los resultados obtenidos permiten acotar el origen de cada miembro dolomítico, aportando nuevos datos geológicos en el Prebético. Dichos cuerpos se agrupan en: i) dolomías estratiformes de gran extensión hospedadas en calizas del Jurásico Inferior y Medio, así como del Cretácico Superior; ii) dolomías de tipo estratiforme y en forma de parches hospedadas en una secuencia carbonatada del Jurásico Superior al Cretácico inferior. El origen de estas dolomitizaciones se atribuye a: i) interacción con agua marina presumiblemente a baja temperatura (dolomías estratiformes de gran extensión); ii) presencia de salmueras hidrotermales de alta temperatura (dolomías estratiformes y parcheadas). Estos resultados pueden servir de guía para otras áreas dolomitizadas poco estudiadas en la zona del Prebético.*

Palabras clave: *dolomía, isótopos estables, Prebético, Riópar.*

INTRODUCCIÓN

Dolostone formation has been linked with different geological processes and settings and after more than two hundred years of intensive research their origin is still controversial (Machel, 2004), although most authors agree that dolomite is rarely precipitated as a primary phase. Various dolomitization models have been proposed by a large number of workers (e.g. Warren, 2000). In essence, the resulting dolostones can be classified as low temperature, referring to those formed from cold Mg-seawater, or burial dolomites, those formed at slightly to much higher temperatures by other Mg-bearing fluids. Quite commonly it is difficult to unravel their precise origin.

The Prebetic zones (SE Spain) are home to extensive outcrops of dolostones, some of which constitute important Natural Parks with particular landscapes (e.g. Calares del Mundo, Albacete). Several dolostone bodies are hosted in Lower Jurassic to Upper Cretaceous carbonates. Navarro-Ciurana et al. (2016) discussed the origin of the dolomites hosted in Upper Jurassic to Lower Cretaceous carbonates in the Riópar area. However, in their study, these authors did not include the Prebetic dolostones hosted in Lower and Middle Jurassic as well as in Upper Cretaceous carbonates. On the other hand, the geologic maps of the area assign specific ages to these dolostones, assuming that they occurred more o less cogenetically with the host carbonates. These assumptions may lead to geological errors as dolomites can result from secondary geological processes, replacing calcitic host rocks well after the host carbonate formed.

In this contribution, the description of the different Riópar dolostone occurrences together with C and O isotope data are presented. Results constrain the origin of dolomitization processes for each dolomitic unit providing new geologic information on the geologic history of the Prebetic.

GEOLOGICAL SETTING

The studied area is located near the Riópar village, where siliciclastic rocks, limestones and dolostones occur. This area is situated at the limit between the External and Internal Prebetic Zones, in the outer portion of the NNW-verging fold-and-thrust belt of the Betic Cordillera (e.g. García-Hernández et al., 1980). The Prebetic is dominated by a Mesozoic to Cenozoic sedimentary sequence up to 2000 m thick, originally deposited in the southern part of the Iberian continental paleomargin (Vera et al., 2004). The External Prebetic Zone shows extensively exposed Triassic and Jurassic rocks and scarcity of Cretaceous and Paleogene sediments. In contrast, the Internal Prebetic Zone is characterized by absence of Triassic rocks, scarcity of Jurassic strata and extensively exposed Cretaceous and Paleogene sediments (Vera et al., 2004).

From a tectonic standpoint, the Prebetic Zones are characterized by the Cazorla-Alcaraz-Hellín structural arc (Rodríguez-Estrella et al., 1979). In general, it is constituted by two major fault systems: i) NE-SW to E-W trending and SE- to S-dipping Alto Gualdalquivir-San Jorge fault; and ii) NW-SE to W-E trending Socovos-Calasparra dextral strike-slip fault perpendicular to the fold axes. These is thought to separate the Internal Prebetic (to the S) from the External Prebetic (to the N) zones (Fig. 1).

In the Riópar area a large number of Mesozoic sedimentary units can be observed (Fig. 2). Triassic sandstones with clays and gypsum and Lower to Middle Jurassic carbonates crop out in the N block of the Socovos fault, whereas carbonates of Upper Cretaceous age appear in the S block of the San Jorge fault. Upper Jurassic to Lower Cretaceous age carbonates crop out between the two faults.

OCURRENCE OF DOLOSTONE GEOBODIES

Several dolomitized carbonates are identified in the Riópar area. Their distribution along the stratigraphic section are illustrated in Figure 2.

Lower Jurassic stratabound dolomites

The Lower Jurassic stratabound dolomitized Carretas and partly Contreras-Madroño limestone Fms. (Fig. 2) are characterized by red to grey colors. The thickness of these formations exceeds 150 m in the Riópar area. They are constituted by microcrystalline subhedral to euhedral (planar-s to planar-e) replacive dolomite crystals, showing a massive aspect in hand samples. At the top of the sequence, non-dolomitized fossiliferous intra-pelsparitic and intra-oosparitic grainstones to packstones, and intra-pelmicritic wackstones to mudstones occur. The dolomitization is mainly fabric-retentive, as oolitic allochems and porosity of precursor limestones are recognized, preserving the original depositional fabrics (i.e., stratification).

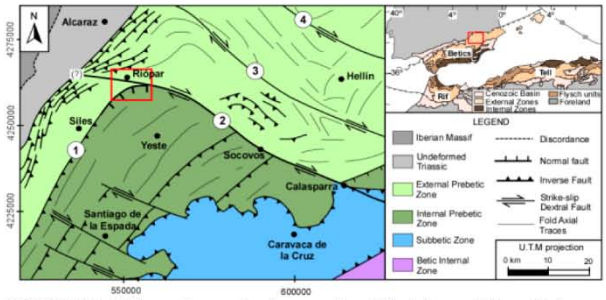

FIGURE 1. *Schematic geologic map (modified from: Pérez-Valera et al., 2010) of the Prebetic Zones and Riópar area: (1) Alto Guadalquivir-San Jorge fault; (2) Socovos fault; (3) Liétor fault; and (4) Pozohondo fault.*

Middle Jurassic stratabound dolomites

The Middle Jurassic stratabound dolomitized limestones, which replace the Chorro carbonate Fm. (Fig. 2), are characterized by white colors in more than 250 m thick sediments in the studied area. They are constituted by fine to coarse planar-e sucrosic dolomite crystals, which replace fossiliferous intra-oosparitic grainstones to packstones and to a lesser extend, mudstones. The replacement is fabric-retentive as oolitic ghosts can be identified, although original sedimentary structures, such as stratification, are rarely preserved.

Upper Jurassic to Lower Cretaceous stratabound and patchy dolomitized carbonates

Stratabound dolostones connected by patchy dolostone bodies are hosted in the Upper Jurassic to the Lower Cretaceous carbonate succession (Fig. 2). In the Riópar area, they outcrop over an area of 4.6 km^2 between San Jorge and Socovos faults.

Two stratabound dolostones are identified replacing intra-oosparitic grainstones to packstones and mudstones of the Lower and Upper Members of Sierra del Pozo Fm. respectively, preserving the original depositional fabrics. They are constituted by microcrystalline planar-s to planar-e replacive dolomite crystals. The Lower Mb. is partially dolomitized as it preserves oolitic limestone lenses; the dolostones contain abundant oolitic ghosts. However, the Upper Mb. has always been observed completely dolomitized, only showing abundant orbitolinid moldic porosity.

Different patchy dolostones have been mapped affecting the Lower Mb. of Sierra del Pozo to the Arroyo de los Anchos Fm. They are constituted by planar-e sucrosic dolomite crystals and fine to coarse non-planar saddle dolomites. The patchy dolomitization fronts are irregular and gradual with the stratabound dolostone units, obliterating the sedimentary fabrics. Nevertheless, the contact with the undolomitized carbonates is sharp, cross-cutting bedding and stratification. Moreover, patchy dolostone outcrops nearer the San Jorge than Socovos strike-slip dextral fault, suggesting a structural control for these dolomitization (Navarro-Ciurana et al. 2016).

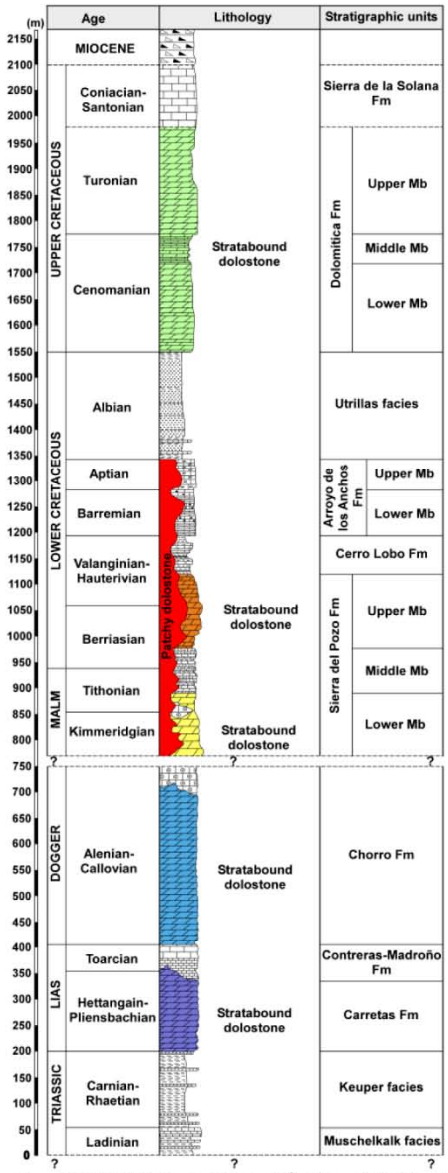

FIGURE 2. *Stratigraphic section of the Riópar area with sedimentary units and location of the studied dolostone geobodies.*

Upper Cretaceous stratabound dolomites

The Upper Cretaceous stratabound dolomitized Cenomanian to Turonian limestones (Fig. 2) are formed by fine planar-s to planar-e dolomite crystals. They are characterized by three different zones: i) the lower part, which is constituted by ochre dolostones with orbitolinid ghosts; ii) the middle zone, formed by white dolostones with oolitic ghosts and interbedded thin dolomitic marls; and iii) the uppermost part, which is constituted by grey dolostones. The thickness of these formations exceeds 250 m in the Riópar area.

C AND O ISOTOPE DATA

Samples of host limestones and dolomite crystals were analyzed for their carbon and oxygen isotope composition (Fig. 3). The isotopic signature of non-dolomitized limestones of Jurassic to Cretaceous age ranges from +0.5 to +3.2‰ for $\delta^{13}C_{V\text{-}PDB}$ and from +27.6 to +30.9‰ for $\delta^{18}O_{V\text{-}SMOW}$. These values are compatible with carbonates precipitated from seawater of Jurassic to Cretaceous age (Veizer et al., 1999).

Stratabound dolostones hosted in Lower and Middle Jurassic limestones have $\delta^{13}C_{V\text{-}PDB}$ values from +3.2 to +3.8‰ and $\delta^{18}O_{V\text{-}SMOW}$ from +29.0 to +29.8‰. Stratabound and patchy dolostones hosted in Upper Jurassic and Lower Cretaceous limestones show similar C and O isotope values ($\delta^{13}C_{V\text{-}PDB}$: -2.3 to +0.8‰; $\delta^{18}O_{V\text{-}SMOW}$: +25.1 to +27.6‰), although stratabound dolostone shows more restricted C isotope values ($\delta^{13}C_{V\text{-}PDB}$: +0.0 to +0.6‰) than patchy dolostones. On the other hand, the isotopic signature of dolomitized Upper Cretaceous limestones ranges from +2.5 to +2.7‰ for $\delta^{13}C_{V\text{-}PDB}$ and from +26.9 to +29.5‰ for $\delta^{18}O_{V\text{-}SMOW}$.

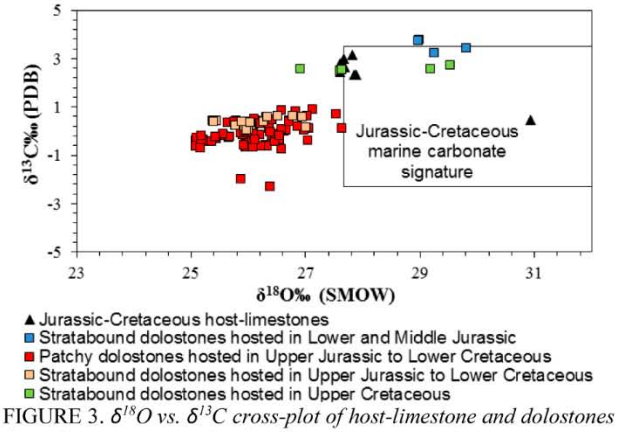

FIGURE 3. *$\delta^{18}O$ vs. $\delta^{13}C$ cross-plot of host-limestone and dolostones from the Riópar area (Prebetic) with a Jurassic-Cretaceous marine carbonate box according to Veizer et al. (1999).*

ORIGIN OF DOLOSTONE GEOBODIES

Sparse remains of fauna (e.g., orbitolinids) and oolitic and peloidal ghosts in thin sections suggest that the Riópar dolostones replace an original marine limestone. Textures and isotopic data support a seawater dolomitization model for the large stratabound dolomite bodies hosted in the Lower and Middle Jurassic and Upper Cretaceous limestones. However, for the stratabound dolostones connected by patchy geobodies and hosted in the Upper Jurassic to Lower Cretaceous carbonate succession, a fault-controlled hydrothermal dolomitization model is favored (Navarro-Ciurana et al., 2016).

The C and O isotopic values of the Lower and Middle Jurassic and Upper Cretaceous dolostones are similar to data of Jurassic to Cretaceous host-limestones. Moreover the carbon and oxygen data of dolostones are within the range of Jurassic to Cretaceous marine carbonates (Veizer et al., 1999), supporting a seawater dolomitization model, which commonly involve lower temperatures of precipitation (Warren, 2000). These three separated stratabound dolostone geobodies probably formed just after the diagenesis of host-limestones, as grain component dissolution (e.g., orbitolinids and ooids) occurred previous to dolomitization.

The C and O isotopic distribution of Upper Jurassic to Lower Cretaceous stratabound and patchy dolomitized limestones depicts a horizontal trend with a small $\delta^{13}C$ (≈2‰) and $\delta^{18}O$ (≈3.5‰) shift. Compared to the host-limestone, these dolostones show relatively depleted $\delta^{13}C$ and $\delta^{18}O$ values. This distribution can be modeled from an interaction of regional carbonates ($\delta^{13}C_{V\text{-}PDB}$: +2.3‰; $\delta^{18}O_{V\text{-}SMOW}$: +28.3‰) with a hydrothermal fluid ($\delta^{13}C_{V\text{-}PDB}$: -8‰; $\delta^{18}O_{V\text{-}SMOW}$: +17‰). Microthermometrical data (Navarro-Ciurana et al., 2016) from stratabound and patchy dolostones (T_h: 150-250ºC; salinity: 5-25 wt.% eq. NaCl) supports the presence of hot dolomitizing brines. Tectonic and stratigraphical considerations suggest that hydrothermal fluids probably circulated upwards through the San Jorge fault.

REGIONAL SCALE IMPLICATIONS

Field and petrographic observations only, do not allow in differentiating the dolostone units or to determine the dolomite types in the Riópar area. Instead, stable isotopic data turned out to be useful to differentiate the dolomitic units (Fig. 3). The area comprised between the Socovos and San Jorge faults in the Riópar zone, had previously been considered and mapped as Middle Jurassic dolostones (Fernández-Gianotti et al., 2001). Nevertheless, we observed clear evidences that this zone is constituted by dolostones that replace a Middle Jurassic to Lower Cretaceous carbonate sequence (e.g., orbitolinid moldic porosity) by fault-controlled hydrothermal processes. The textures of these dolostones (i.e., sucrosic aspect, presence of oolitic ghosts) are very similar to those of dolostones hosted in Middle Jurassic carbonates, leading to confusions between them. Commonly, the dolostones that outcrop in the footwall block of the Alto Guadalquivir-San Jorge fault in the External Prebetics are interpreted as Middle Jurassic in age. From the data presented here, a revision of these dolostones is suggested, as at least some of them could be of hydrothermal origin.

CONCLUSIONS

The petrographic characterization of the different dolostone occurrences at Riópar together with C and O isotope data constrains the origin of the different dolomitic units: i) seawater dolostones originated presumably at low temperatures (Lower and Middle Jurassic and Upper Cretaceous stratabound dolomitized limestones); and ii) hydrothermal dolostones originated by hot dolomitizing brines (Upper Jurassic to Lower Cretaceous stratabound combined with patchy dolomitized carbonates). Further studies of dolostones at the footwall block of the Alto Guadalquivir-San Jorge fault, assumed to be of Middle Jurassic age should be carried out. The combination of petrographical and isotope studies may be a useful tool to reassess their origin.

ACKNOWLEDEMENTS

This research has been supported by the Spanish *Ministerio de Economía y Competitividad*, through the CGL2011-26488 project.

REFERENCES

Fernández-Gianotti, J., Perucha, M.A, Benito, M.I., Rodríguez-Estrella, T., Nozal, F., Gómez-Fernández, J.J., A. Meléndez, J.J, Aragón, R. and Hornero, J. (2001): *Mapa Geológico de España 1:50.000, hoja nº 866 (Yeste)*. IGME, Madrid.

García-Hernández, M., López-Garrido, A.C., Rivas, P., Sanz de Galdeano, C. and Vera, J.A. (1980): Mesozoic paleogeographic evolution of the external zones of the Betic Cordillera. *Geology en Mijnbouw*. 50 (2): 155-168.

Machel, H.G. (2004): Concepts and models of dolomitization: A critical reappraisal. In: *The Geometry and Petrogenesis of Dolomite Hydrocarbon Reservoirs* (Braithwaite C.J.R., Rizzi, G. and Darke. G., eds.). Geological Society of London Special Publications, 235, 7-63.

Navarro-Ciurana, D., Corbella, M., Cardellach, E., Vindel, E., Gómez-Gras, D. and Griera, A. (2016): Petrography and geochemistry of fault-controlled hydrothermal dolomites in the Riópar area (Prebetic Zone, SE Spain). *Marine and Petroleum Geology*. 71: 310-328.

Pérez-Valera, L.A., Sánchez-Gómez, M., Fernández-Soler, J.M., Pérez-Valera, F. and Azor, A. (2010): Diques de lamproítas a lo largo de la falla de Socovos (Béticas orientales). *Geogaceta* 48: 151-154.

Rodríguez-Estrella, T. (1979): Geología e hidrogeología del Sector de Alcaraz-Liétor-Yeste (Provincia de Albacete). Instituto Geológico y Minero de España 97, 566.

Veizer, J., Ala, D., Azym, K., Bruckschen, P., Buhl, D., Bruhn, F., Carden, G.A.F., Diener, A., Ebneth, S., Godderis, Y., Jasper, T., Korte, C., Pawellek, F. and Podlaha, O. (1999): $^{87}Sr/^{86}Sr$, $\delta^{13}C$ and $\delta^{18}O$ evolution of Phanerozoic seawater. *Chemical Geology*. 161: 59-88.

Vera, J.A., Arias, C., García-Hernández, M., López-Garrido, A.C., Martín-Algarra, A., Martín-Chivelet, J., Molina, J.M., Rivas, P., Ruiz-Ortiz, P.A., Sanz de Galdeano, C. and Vilas, L. (2004). Las Zonas Externas Béticas y el paelomargen Sudibérico. In: *Geología de España* (Vera, J.A., ed.). Sociedad Geológica de España e Instituto Geológico de España, 354-360.

Warren, J. (2000): Dolomite: occurrence, evolution and economically important associations. *Earth-Science Reviews*. 52: 1-81.

ANEXO

2

Relación entre las texturas de la dolomita y la temperatura de formación – conocimientos sobre el área de Riópar (Cuenca Bética, SE de España)

MADRID 2015
1-4 June 2015 I IFEMA Madrid

Tu N110 07

Relationship between Dolomite Textures and Formation Temperature - Insights from the Riópar Area (Betic basin, SE Spain)

D. Navarro-Ciurana* (Universitat Autònoma de Barcelona), M. Corbella (Universitat Autònoma de Barcelona), D. Gómez-Gras (Universitat Autònoma de Barcelona), A. Griera (Universitat Autònoma de Barcelona), E. Vindel (Universidad Complutense de Madrid), L. Daniele (Universidad de Chile) & E. Cardellach (Universitat Autònoma de Barcelona)

SUMMARY

This study reports textures and homogenization temperatures of primary fluid inclusions on dolomites hosted in Upper Jurassic to Lower Cretaceous age carbonate sequence from the Riópar area (Mesozoic Prebetic Basin, SE Spain). Five dolomite texture-types have been identified: i) planar subhedral replacive dolomite (ReD); ii) transition between planar subhedral to euhedral dolomite (ReD-SuD); iii) planar euhedral sucrosic dolomite (SuD); iv) non-planar cloudy saddle dolomite (SaD-I); and v) non-planar clear saddle dolomite (SaD-II). Fluid inclusions in ReD-SuD dolomite show a Th mode value of 205ºC, while SaD-I and SaD-II show Th mode values of 235ºC and 195ºC respectively. Our research indicates that planar and non-planar dolomite textures are formed at high-temperatures under hydrothermal conditions in deep-burial diagenetic environments, unsupporting the accepted idea that planar dolomites are formed under temperatures around or less than 50-60ºC in shallow-burial diagenetic environments.

MADRID 2015
1-4 June 2015 I IFEMA Madrid

Introduction

Dolomitic rocks constitute a potential natural resource as they may host large amounts of economic base-metals (i.e. Zn-Pb-F ore-deposits: Leach and Sangster, 1993) and more than half of the world's hydrocarbon reserves (e.g. Warren, 2000). In addition, dolomitization processes have long been an interesting topic for mineral and oil resource exploration and production.

Dolostones are usually classified according to crystal size, texture, fabric, distribution and shape (Friedman, 1965; Randazzo and Zachos, 1984). Gregg and Sibley (1984) and Sibley and Gregg (1987) proposed a classification of dolomite textures according to crystal growth effects (planar or non-planar) and the degree of dolomitization based on their formation temperature. According to different authors (e.g. Lewis, 1980), the growth temperature of dolomite is one of the main factors affecting dolomite textures. Typically, the limit between planar and non-planar dolomite formation temperature is reported in the 50 to 60ºC range (Gregg and Sibley, 1984; Sibley and Gregg, 1987). Planar dolomite is assumed to precipitate during early diagenesis at temperatures around or lower than 50-60ºC in shallow-burial environments (Machel, 2004). On the other hand, the precipitation of non-planar dolomite usually occurs at higher temperatures, commonly under deep-burial diagenetic conditions (Warren, 2000). Also, non-planar saddle dolomite, characterized by curved crystal faces and wavy extinction, is thought to precipitate from hydrothermal fluids under a temperature range from 80 to 150ºC and exceptionally up to 200ºC (Machel, 2004). Nevertheless, evidence from microthermometric data of fluid inclusions (FIs) do not support this view (e.g. Huang et al., 2014). Homogenization temperatures around 120ºC in planar euhedral dolomites crystallized after circulation of hydrothermal fluids along major faults from the Asón valley (Basque-Cantabrian Basin, N Spain) have been reported by López-Horgue et al. (2010).

This research discusses the relationship between dolomite textures, described according to Gregg and Sibley (1984) and Sibley and Gregg (1987) textural classification, and dolomite temperature formation and diagenetic environment. The studied samples were collected in the Riópar area, located at the limit between Internal and External Prebetic Zones (N boundary of the Mesozoic Betic Rift, SE Spain). Dolostones are hosted in Upper Jurassic to Lower Cretaceous age carbonates and related to Zn-Pb occurrences.

Methodology

Petrographical and cathodoluminiscence (CL) study was performed on 145 polished-thin sections. Staining with alizarine red-S and potassium ferricyanide was used to differentiate calcite from dolomite and their ferroan equivalents. A Technosyn Cold Cathodoluminescence 8200 MarkII device, operating at 15-18 Kv and 150-350 µA gun current, was used for CL study at the *Dpt. de Geoquímica, Petrologia i Prospecció Geològica* of the *Universitat de Barcelona*. Microthermometry measurements were conducted on double-polished 50-µm-thick sections and carried out using a Linkam THMS-600 heating-freezing stage at the *Dpt. de Geologia* of the *Universitat Autònoma de Barcelona*.

Dolomite textures

Planar-s replacive dolomite (ReD) is characterized by a brownish to grayish color on weathered surfaces. Under microscope (Fig. 1a), it shows lowly to densely packed equigranular dolomite with crystal sizes ranging from 10 to 30 µm. Dolomite shapes are mostly subhedral with cloudy appearance (inclusion-rich) showing oval and serrated crystal boundaries. Transitions of planar subhedral to euhedral dolomites (ReD-SuD) are frequent, showing crystal sizes from 10 to 50 µm (Fig. 2a). Most crystals are cloudy under plane polarized light with dominant straight extinction under cross polarized light. These dolomites are slightly ferroan as indicated by its pale blue color staining and have a characteristic homogenous bright red luminescence (Fig. 1a). ReD is pervasively replacive, which is evidenced by the presence of original limestone ghosts, predominantly micritized ooids (Fig. 1a) and in a lesser extent, peloids and intraclasts.

Planar-e sucrosic dolomite (SuD) is characterized by its whitish color in fresh rock. Under microscope examinations, it shows very lowly to densely packed inequigranular crystals with medium to coarse sizes (250 µm to 2 mm: Fig. 1b). Micrometer intercrystalline and milimeter to centimeter vuggy porosity is well developed (around 15%). This dolomite type is euhedral with rhombohedral morphologies showing mainly cloudy (inclusion-rich) centers and clear (inclusion-poor) borders (Fig. 2b) and straight extinction under crossed light. It is non-ferroan to slightly ferroan as indicated by the non-staining to pale blue staining. The clear crystal borders show dull red and bright orange luminiscense rims (Fig. 1b). SuD occurs as: i) ReD recrystallizations, evidenced by the presence of cloudy crystals centers that correspond to precursor dolomite ghosts with bright red luminescence (Fig. 1b); and ii) ReD overgrowths, showing irregular boundaries and crystal size increase.

Non-planar saddle dolomite (SaD) show slightly curved faces and sweeping extinction under cross polarized light. Two saddle dolomite-types have been identified: cloudy (SaD-I) and clear (SaD-II) saddle dolomites. SaD-I is composed of lowly to densely packed equigranular crystals with fine- to medium-sized (50 µm to 5 mm: Fig. 1c) and cloudy appearance (inclusion-rich: Fig. 2c). It is non-ferroan to slightly ferroan. Under CL, SaD-I shows growth zoning with bright to dull-dark red alternations (Fig. 1c). SaD-II forms lowly to densely packed inequigranular crystals with coarse- to very coarse-sized (500 µm to 1 cm: Fig. 1d). It always occurs as zoned crystals showing cloudy (inclusion rich) and clear (inclusion poor) alternating rims (Fig. 2d) and is non-ferroan to ferroan. The cloudy and clear rims show strong growth zoning with bright orange to red, dull-dark red and non-luminiscene alternating bands (Fig. 1d). SaD-I pre-dates Zn-Pb sulfides, whereas SaD-II fill remnant porosity after SaD-I and sulfide precipitation (Fig. 1d). SaD dolomite occurs as: i) ReD and SuD recrystallizations, showing gradual transitions (Fig. 1c); ii) ReD and SuD overgrowths, with irregular transitional contacts and gradual grain size increases; iii) millimetric to centimetric veins that crosscut the previous dolomites; and iv) cementing dolostone clasts in breccias.

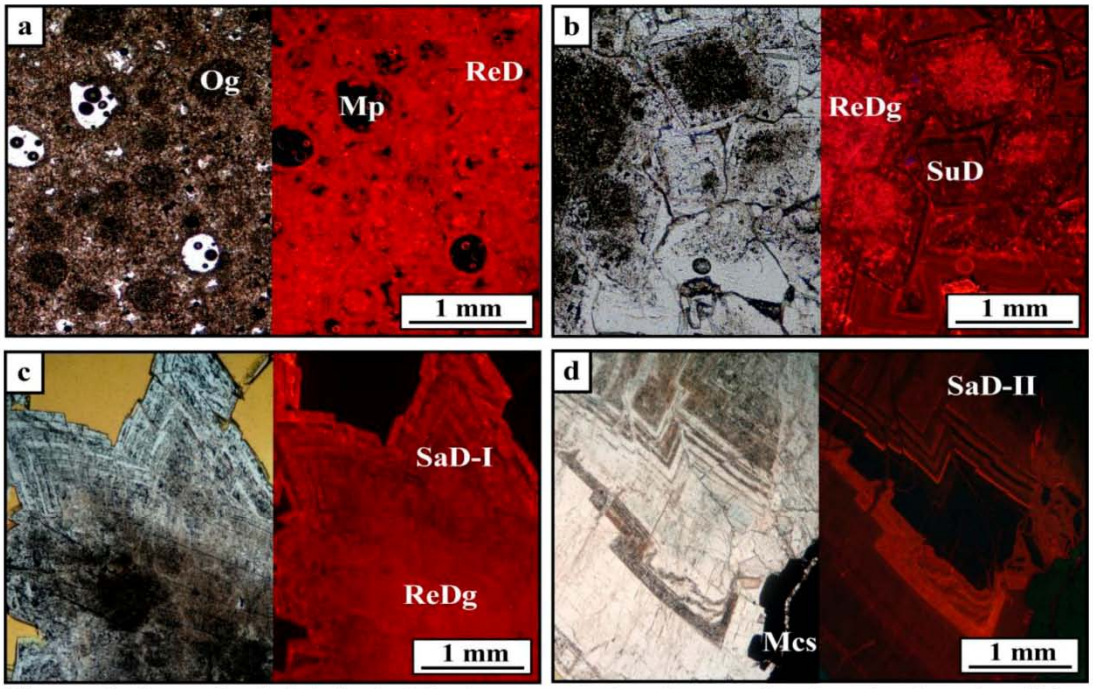

Figure 1 *Transmitted light/cathodoluminescence microphotograph-pairs showing the Riópar dolomite textures:* ***a)*** *planar-s replacive dolomite (ReD);* ***b)*** *planar-e sucrosic dolomite (SuD);* ***c)*** *non-planar cloudy saddle dolomite (SaD-I); and* ***d)*** *non-planar clear saddle dolomite (SaD-II). Mp: moldic porosity; Og: ooid ghost; ReDg: planar-s replacive dolomite ghost; Mcs: marcassite.*

MADRID 2015
1-4 June 2015 I IFEMA Madrid

The dolomitization sequence at Riópar is represented by fine planar-s replacive dolomite that evolved to planar-e sucrosic and ended with a non-planar saddle dolomite. Crystal size increases with time. Three dolomite occurrence-types have been observed: replacements, recrystallizations and overgrowths pore-space filling.

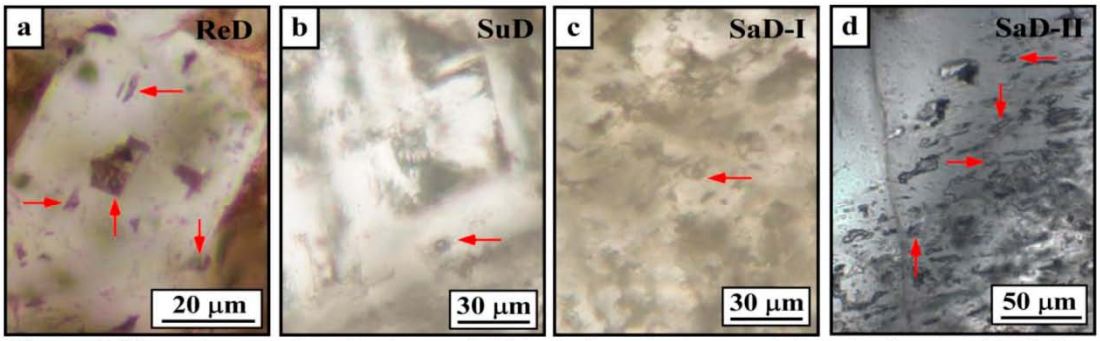

Figure 2 *Photomicrographs of primary fluid inclusions (red arrows) in:* ***a)*** *planar subhedral to euhedral dolomite (ReD-SUD);* ***b)*** *sucrosic dolomite (SuD);* ***c)*** *saddle cloudy dolomite (SaD-I); and* ***d)*** *saddle clear dolomite (SaD-II).*

Fluid inclusion data

Homogenization temperatures (T_h) were measured on primary fluid inclusions from ReD-SuD transitional, SaD-I and SaD-II dolomites. No T_h measurements on ReD and SuD FIs could be performed. Two-phase (liquid-vapor) fluid inclusions (FIs) were found in crystal cores of ReD-SuD (Fig. 2a), in concentric growth-zones of SuD and SaD-II (Fig. 2b and 2d) and throughout individual crystals in SaD-I (Fig. 2c). FIs are irregular to elongate in shape with sizes ranging from 3 to 15 µm and variable vapor/liquid ratios (5 to 25). T_h values on ReD-SuD range from 189 and 240ºC, with a mode of 205ºC (1σ, *n*=14). SaD-I and SaD-II show T_h values between 178 to 247ºC with a mode of 235ºC (1σ, *n*=24) and 156 to 236ºC, with a mode of 195ºC (1σ, *n*=26) respectively (Fig. 3).

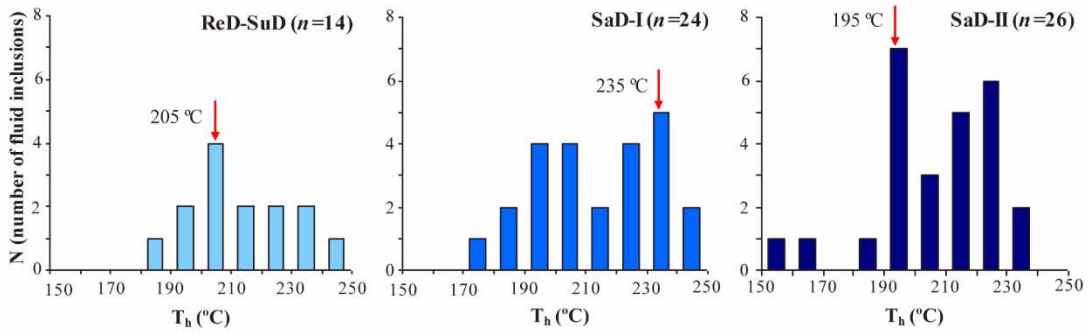

Figure 3 *T_h histograms of different dolomite generations (red arrows: T_h mode).*

An interesting finding in this study is the presence in the Riópar area of high temperature hydrothermal fluids (~205ºC) during the formation of ReD-SuD planar dolomite as observed by Huang et al. (2014) on dolomites from the Sichuan and Tarim Basins in China. This is in contradiction with the usually accepted idea of planar dolomite formation under low-T conditions (Gregg and Sibley, 1984; Sibley and Gregg, 1987). These temperatures are similar to those found in non-planar saddle dolomites (SaD-I: ~235ºC; SaD-II: ~195ºC), suggesting a unique hot dolomitizing fluid that evolved with time. According to Warren (2000) these high-temperatures are typical of deep-burial diagenetic environments. The spread of T_h values obtained in the studied dolomites might be related either to recrystallization phenomena or to mixing between fluids of contrasting temperatures. In any case, even the lower temperatures obtained are well above those reported for planar dolomite formation conditions elsewhere (e.g. Gregg and Sibley, 1984; Sibley and Gregg, 1987).

Conclusions

Primary fluid inclusion data from Riópar dolomites put constraints and give a new insight on the relationship between dolomite textures, formation temperature and diagenetic environment, unsupporting the accepted idea that planar dolomites form under temperatures around or less than 50-60ºC in shallow-burial diagenetic environments. Even though more work is needed to generalize this observation, the following conclusions can be drawn: i) high T_h´s of fluid inclusions in planar (ReD-SuD: ~205ºC) and non-planar saddle (SaD-I: ~235ºC; SaD-II: ~195ºC) dolomites confirm the presence of a hot fluid responsible for the dolomitization under hydrothermal conditions; ii) petrographic observations of dolomite textures do not always provide a quick and easy way to determine their temperature formation and the diagenetic environment; iii) temperature and burial diagenetic environment may not be the principal control of dolomite textures; and iv) a revision of the accepted dolomite classification proposed by Greeg and Sibley (1984) and Sibley and Gregg (1987), which relates planar dolomite texture with relatively low temperatures under shallow-burial diagenetic environments, as suggested by Warren (2000) and Machel (2004), is necessary.

Acknowledgements

This research has been supported by the Spanish Ministry of Economy and Competitive, through the CGL2011-26488 project.

References

Friedman, G.M. [1965] Terminology of crystallization textures and fabrics in sedimentary rocks. *Journal of Sedimentary Petrology*, **35**, 643-655.

Gregg, J.M. and Sibley, D.F. [1984] Epigenetic dolomitization and the origin of xenotopic dolomite texture. *Journal of Sedimentary Research*, **54**(3), 908-931.

Leach, L.A. and Sangster, D.F. [1993] Mississippi Valley-type lead-zinc deposits. In; Kirkham R.V., Sinclair, W.D., Thorpe, R.I., and Duke, J.M. (Eds.) Mineral deposit modeling. Geological Association of Canada Special Paper, **40**, 289-314.

Lewis, B [1980] Nucleation and growth theory. In; Pamplin, B.R. (Ed.) Crystal Growth. Pergamon Press, Oxford, 23-63.

López-Horgue, M.A., Iriarte, E., Schröder, S., Fernández-Mendiola, P.A., Caline, B., Corneyllie, H., Frémont, J., Sudri, M. and Zerti, S. [2010] Structurally controlled hydrothermal dolomites in Albian carbonates of the Asón valley, Basque Cantabrian Basin, Northern Spain. *Marine and Petroleum Geology*, **27**(5), 1069-1092.

Machel, H.G. [2004] Concepts and models of dolomitization: A critical reappraisal. In; Braithwaite C.J.R., Rizzi, G. and Darke. G. (Eds.) The Geometry and Petrogenesis of Dolomite Hydrocarbon Reservoirs. *Geological Society of London Special Publications*, **235**, 7-63.

Randazzo, A.F. and Zachos, L.G. [1984] Classification and description of dolomitic fabrics of rocks from the Floridan aquifer, USA. *Sedimentary Geology*, **37**, 151-162.

Sibley, D.F. and Gregg, J.M. [1987] Classification of dolomite rock texture. *Journal of Sedimentary Petrology*, **52**, 1087-1100.

Huang, S., Huang, K., Lü, J. and Lan Y. [2014] The relationship between dolomite textures and their formation temperature: a case study from the Permian-Triassic of the Sichuan Basin and Lower Paleozoic of the Tarim Basin. *Petroleum Science*, **11**, 39-51.

Warren, J. [2000] Dolomite: occurrence, evolution and economically important associations. *Earth-Science Reviews*, **52**, 1-81.

ANEXO

3

REE e isótopos de Sm-Nd como indicios de interacción fluido-roca a alta temperatura en la dolomitización de Riópar (SE de España)

Available online at www.sciencedirect.com

ScienceDirect

Procedia Earth and Planetary Science 00 (2017) 000–000

Procedia
Earth and Planetary Science

www.elsevier.com/locate/procedia

15th Water-Rock Interaction International Symposium, WRI-15

REE and Sm-Nd clues of high-temperature fluid-rock interaction in the Riópar dolomitization (SE Spain)

Dídac Navarro-Ciurana[a]*, Esteve Cardellach[a], Carmen Galindo[b], José Manuel Fuenlabrada[c], Albert Griera[a], David Gómez-Gras[a], Elena Vindel[d], Mercè Corbella[a]

[a]*Departament de Geologia, Facultat de Ciències, Universitat Autònoma de Barcelona, Edifici Cs s/n, Bellaterra 08193, Spain*
[b]*Departamento de Petrología y Geoquímica e Instituto de Geociencias, Universidad Complutense de Madrid-CSIC, c/ José Antonio Novais 12, Madrid 28040, Spain*
[c]*CAI de Geocronología y Geoquímica Isotópica, Facultad de Ciencias Geológicas, Universidad Complutense de Madrid, c/ José Antonio Novais 2, Madrid 28040, Spain*
[d]*Departamento de Cristalografía y Mineralogía, Facultat de Ciencias Geológicas, Universidad Complutense de Madrid, c/ José Antonio Novais 12, Madrid 28040, Spain*

Abstract

REE geochemistry and Sm-Nd isotope data of Mesozoic stratabound and patchy dolostones of the Riópar area (Prebetic Zone, SE Spain) are presented. The results, combined with previously published data, suggest the dolomitizing fluid was a warm brine that interacted with siliciclastic rocks of Triassic age and with the host carbonates at low fluid-rock ratios. The positive Eu anomaly, negative εNd values and MREE patterns confirm that the dolostones were formed by interaction with warm acidic crustal fluids. C-O isotopic interaction models indicate that these fluids were characterized by $\delta^{18}O$-enriched and $\delta^{13}C$-depleted compositions, pointing to low ratios of fluid to rock volumes. The studied dolostones show two Sr sources: one Sr signature is close to the host carbonate values and the other one is more radiogenic, indicating that fluids became enriched in ^{87}Sr after interacting with siliciclastic rocks. Furthermore, the Sr-Nd isotope data systematic depicts a positive correlation, thus probably the same rock sources are shared for both elements. Moreover, the warm fluids interacted with regional limestones achieving a negative Ce and positive La anomalies, low $\delta^{18}O$ compositions and similar $\delta^{13}C$ values than the host carbonates.

Peer-review under responsibility of the organizing committee of WRI-15.

Keywords: geochemistry; rare earth elements; stable and radiogenic isotopes; water-rock interection; Riópar hydrothermal dolomites.

* Corresponding author. Tel.: +34-93-581-4773.
E-mail address: didac.navarro.ciurana@gmail.com

Peer-review under responsibility of the organizing committee of WRI-15.

1. Introduction

The study of dolostones and dolomitizing processes is of a great interest as the resulting rocks may host economic base-metal (Zn-Pb-F) ore-deposits and host more than half of the world's hydrocarbon reserves[1]. Dolostone formation has been linked with different geological processes and settings, but after more than two hundred years of intensive research, their origin is still controversial[1]. Most of the existing dolostone case studies are based on detailed petrographic descriptions, geochemical data analyses of trace elements and of the isotopic compositions of oxygen, carbon, and strontium to gain insight into dolomitization processes[2]. Although not as widely applied as previous analyses, rare earth elements (REE) and the Sm-Nd isotopic system are increasingly used as proxies in order to understand the flow controls and the origin of fluids involved on the dolomite formation in diagenetic environments[2].

In the Riópar area (Prebetic, SE Spain) dolomitized bodies replace Upper Jurassic to Lower Cretaceous carbonatic rocks. Detailed descriptions of the different dolostone geobodies, dolomite phases as well as geochemical data (major element composition, C/O and Sr isotopes) and fluid inclusions microthermometrical analyses were reported by Navarro-Ciurana et al.[3]. The present study incorporates REE and Sm-Nd isotope geochemistry into the analysis of Riópar dolostones; to our knowledge, this constitutes the first report of this kind focused on carbonate rocks from Iberian Mesozoic basins. The combination of new and previously published data is here used to constrain the type of dolomitizing fluid and sheds light on the fluid-rock interaction during dolomitization.

2. Geological setting and dolomite distribution

Riópar is located at the limit between the External and Internal Prebetic Zones, in the outer portion of the NNW-verging fold-and-thrust belt of the Betic Cordillera (SE Spain). The External Prebetic Zone consists in extensively exposed Triassic siliciclastic sediments and Jurassic carbonate rocks and scarcity of Cretaceous and Paleogene sediments. In contrast, the Internal Prebetic Zone is characterized by broad outcrops of Cretaceous and Paleogene sediments[4]. From a tectonic standpoint, the Prebetic Zones are separated by two major system faults: the Alto Gualdalquivir-San Jorge fault with NE-SW to E-W trending and SE- to S-dipping, and the Socovos-Calasparra dextral strike-slip fault with NW-SE to W-E trending.

In the Riópar area, stratabound and patchy dolostones are found in carbonate rocks from Upper Jurassic to Lower Cretaceous ages, bounded between San Jorge and Socovos faults. Two stratabound bodies respectively replace Kimmeridgian and Upper Berriasian to Valanginian grainstones, packstones and mudstones. They are predominantly constituted by microcrystalline replacive dolomite crystals (ReD). The patchy dolostones affect Kimmeridgian up to Aptian carbonates, also connecting the stratabound bodies. They consist of sucrosic dolomite cements (SuD) and fine to coarse saddle dolomites (SaD). These dolomites outcrop nearer the San Jorge than Socovos faults, suggesting a structural control for this dolomitization (see: Navarro-Ciurana et al.[3]).

3. REE geochemistry characterization

Highest REE concentrations are found in the stratabound dolostones constituted by matrix-replacive dolomite (ReD), which varies between 14.36 and 53.79 ppm. These dolomites are characterized by elevated concentrations of shale-normalized (SN) middle-REE, showing a "MREE bulge". The $(La/La^*)_{SN}$ ratios range from 1.19 to 1.30, $(Pr/Pr^*)_{SN}$ varies between 1.00 and 1.07, $(Ce/Ce^*)_{SN}$ ranges from 0.80 to 0.87, and $(Eu/Eu^*)_{SN}$ falls between 1.07 and 1.35. The average REE_{SN} pattern of ReD shows negative $Ce_{SN,}$ and positive La_{SN} and Eu_{SN} anomalies (Fig. 1).

Sucrosic dolomite cements (SuD) have lower total SN REE contents than matrix-replacive dolomites (Fig. 1a). Their REE concentrations range from 4.56 to 19.44 ppm. These values are characterized by a light-REE enrichment, negative REE slope tendency and a slightly negative Ce_{SN} anomaly and positive La_{SN} and Eu_{SN} anomalies (Fig. 1). The $(La/La^*)_{SN}$ ratios range from 0.97 to 2.23, $(Pr/Pr^*)_{SN}$ falls between 0.99 and 1.03, $(Ce/Ce^*)_{SN}$ varies between 0.67 and 0.97 and $(Eu/Eu^*)_{SN}$ range from 1.11 to 1.45.

Saddle dolomite cements (SaD) contain total REE from 7.26 to 35.03 ppm. This dolomite also depicts an "MREE bulge" (Fig. 1a). The $(La/La^*)_{SN}$ ratio is restricted between 1.19 and 1.55, $(Pr/Pr^*)_{SN}$ ranges from 0.96 to 1.12, $(Ce/Ce^*)_{SN}$ ranges from 0.64 to 0.88 and $(Eu/Eu^*)_{SN}$ varies from 1.20 to 1.44. The average SN REE pattern of SaD samples show overall negative Ce_{SN} and notably positive La_{SN} and Eu_{SN} anomalies (Fig. 1).

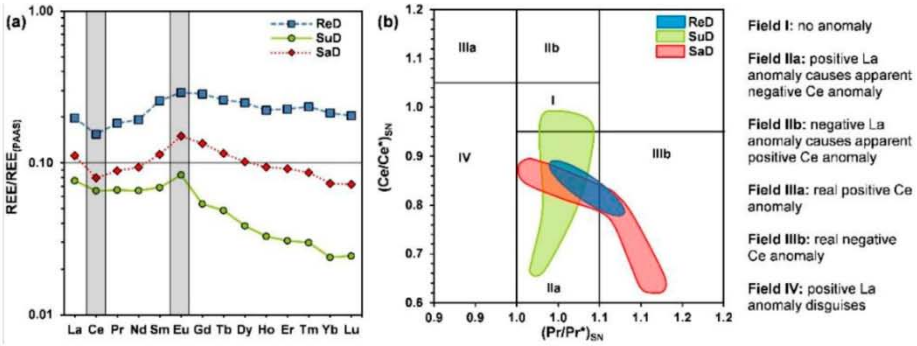

Fig. 1. (a) Average shale-normalized REE patterns of the different Riópar dolomite types against the standard Post-Archean Australian Shale (PAAS)[5]. (b) Cross plot of shale-normalized $(Pr/Pr^*)_{SN}$ versus $(Ce/Ce^*)_{SN}$. ReD: matrix-replacive dolomite; SuD: sucrosic dolomite cement; SaD: saddle dolomite cement.

4. Stable (C and O) and radiogenic (Sr, Sm and Nd) isotope data

The Upper Jurassic to Lower Cretaceous host limestones show $\delta^{13}C$ values between +0.5 and +3.2‰, $\delta^{18}O$ compositions from +27.6 to +30.9‰ and $^{87}Sr/^{86}Sr$ ratios of 0.70723 to 0.70731 (Figs. 2a and 2b)[3]. These values are compatible with carbonates precipitated from seawater of Jurassic to Cretaceous age[6]. According to Navarro-Ciurana et al.[3] stratabound (ReD) and patchy dolostones (SuD and SaD) show similar C and O isotope values ($\delta^{13}C$: -2.3 to +0.8‰; $\delta^{18}O$: +25.1 to +27.6‰) (Fig. 2a) and a $^{87}Sr/^{86}Sr$ ratio that varies from 0.70736 to 0.70830 (Fig. 2b).

The studied dolomite types (ReD and SaD) show restricted $^{147}Sm/^{143}Nd$ (0.112-0.144) and $^{143}Nd/^{144}Nd$ (0.51216-0.51226) isotopic ratios (Fig. 2c). These compositions are not high enough and widespread enough to obtain a reliable isochron from the data. Nevertheless, initial ratios of Nd isotopes can be obtained with an assumption for the oldest age possible: Lower Albian. Recalculations for a geological age of 112 Ma does not alter the Sr isotopic signatures as the Rb concentration in these dolomites appear to be below the detection limit. With this age, the Riópar dolostones display initial $^{143}Nd/^{144}Nd_{(t=112\ Ma)}$ ratios of 0.51207 to 0.51215, and a calculated initial $\varepsilon Nd_{(t=112\ Ma)}$ ranging from -6.7 to -8.2 (Fig. 2c). Although the Nd isotopic concentrations at 112 Ma are lower than the isotopic ratios at actual times, the $^{143}Nd/^{144}Nd$-$^{87}Sr/^{86}Sr$ isotopic relationships show the same distribution pattern for both geologic times (Fig. 2c).

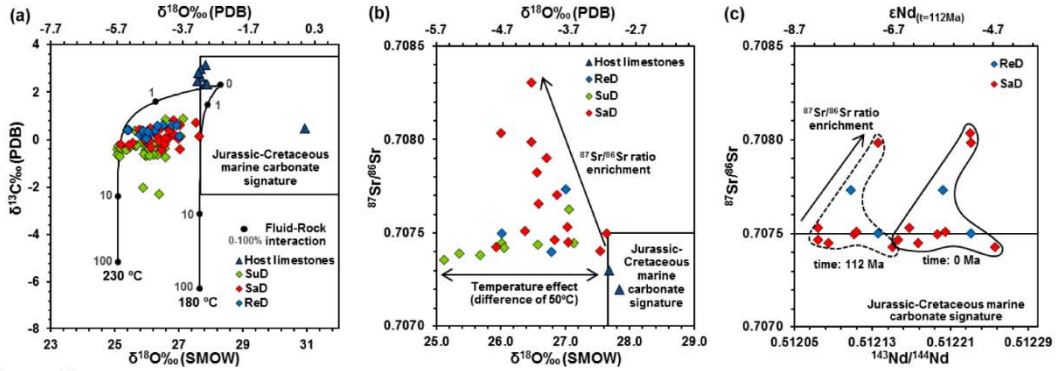

Fig. 2. (a) $\delta^{13}C$ vs $\delta^{18}O$ cross-plot of host limestone and ReD, SuD and SaD dolomite types. C-O isotope model curves were calculated in terms of fluid-rock interaction for dolomite at temperatures of 180 and 230ºC. (b) $\delta^{18}O$ vs $^{87}Sr/^{86}Sr$ cross-plot of host limestone and different dolomites. (c) $^{143}Nd/^{144}Nd$-$^{87}Sr/^{86}Sr$-$\varepsilon Nd_{(t=112\ Ma)}$ cross-plot of ReD and SaD dolomite types at actual times and at an initial age of 112 Ma.

5. Discussion

The positive Eu anomalies (Fig. 1a) of stratabound dolostones could be attributed to hydrothermal alteration from high temperature solutions[7]. This is consistent with microthermometrical data reported by Navarro-Ciurana et al.[3] (T_h=150-250ºC). Moreover, the observed MREE enrichments in the studied matrix-replacive and saddle dolomites (Fig. 1a), suggests the contribution of acidic hydrothermal fluids[8] in the dolostone formation. Using an average T_h value of 205ºC, the C and O isotopic distribution can be modeled as an interaction between the regional limestones and a hydrothermal fluid with an initial isotopic composition of $\delta^{13}C \approx -8‰$ and $\delta^{18}O \approx +17‰$. The data best fits the

interaction at low fluid-rock ratios (Fig. 2a). This $\delta^{18}O$-rich isotopic composition can be achieved by a low $\delta^{18}O$ fluid (i.e. evaporated seawater, residual brines) after isotopic equilibration with carbonates. Furthermore, the narrow $\delta^{13}C$ range of dolostones (Fig. 2a), which is close to the original signature of the host limestones, indicates that the $\delta^{13}C$-depleted composition of the fluid was buffered by the host rocks.

The studied dolostones Sr isotopic signatures point to two sources of Sr, one close to the Jurassic and Cretaceous marine carbonates and another more radiogenic. The latter indicates that the dolomitizing fluid became enriched in ^{87}Sr after circulating and interacting with siliciclastic rocks, most probably of Triassic age due to its abundance in the External Prebetic Zone. Moreover, the LREE enrichment of sucrosic dolomites (Fig. 1a), which is typical of marine limestones with detrital sediment contributions[9], might reflex the interaction between hydrothermal fluids and host limestones and siliciclastic rocks. The Sr and O isotope systematic depicts a trend relating lower $\delta^{18}O$ with higher $^{87}Sr/^{86}Sr$ values (Fig. 2b), pointing to an increase of ^{87}Sr in the fluid as the temperature increases. Furthermore, dolostones display a remarkably small range of $^{147}Sm/^{143}Nd$ and $^{143}Nd/^{144}Nd$ ratios, showing negative εNd values, which is a typical of crustal signature. The Sr and Nd isotope systematics depicts a trend relating higher $^{87}Sr/^{86}Sr$ with higher $^{143}Nd/^{144}Nd$ values (Fig. 2c). This relationship points to the same siliciclastic and shallow marine carbonate rock sources for both radiogenic isotopes.

On the other hand, the Riópar dolostones commonly display light negative Ce and positive La anomalies (Fig. 1). These features are widely regarded as characteristic of marine carbonates formed from oxygen-rich shallow water solutions[10]. Recent studies[11] suggested that unless there is a large amount of diagenetic fluid to flush the system several times through intense water-rock interaction, diagenesis has no significant effect on the composition and distribution of REEs in carbonates. Therefore, the Ce and La anomalies reflect such interaction.

6. Conclusions

Geochemical data (REE, $\delta^{13}C$, $\delta^{18}O$, $^{87}Sr/^{86}Sr$, $^{147}Sm/^{143}Nd$ and $^{143}Nd/^{144}Nd$) from stratabound dolostones connected by patchy dolomite geobodies in the Riópar area (Prebetic Zone, SE Spain) suggests that both dolostone types are formed by acidic crustal hydrothermal fluids ($\delta^{18}O$-enriched and $\delta^{13}C$-depleted) that acquired the radiogenic signature by interaction with siliciclastic rocks. Given the geology of the area, this would be Triassic formations. Furthermore, the warm dolomitizing fluids must have interacted with regional limestones of Jurassic and Cretaceous age at low fluid-rock ratios, consequently buffering the low $\delta^{18}O$ and $\delta^{13}C$ compositions and $^{87}Sr/^{86}Sr$ values to the original marine signature, together with the typical negative Ce and positive La anomalies of the host carbonates.

References

1. Warren J. Dolomite: occurrence, evolution and economically important associations. *Earth-Science Rev.* 2000; **52**: 1-81.
2. Banner JL, Hanson GN, Meyers WJ. Rare earth element and Nd isotopic variations in regionally extensive dolomites from the Burlington-Keokuk Formation (Mississippian); implications for REE mobility during carbonate diagenesis. *J. Sediment. Petrol.* 1988; **58**: 415-432.
3. Navarro-Ciurana D, Corbella M, Cardellach E, Vindel E, Gómez-Gras D, Griera A. Petrography and geochemistry of fault-controlled hydrothermal dolomites in the Riópar area (Prebetic Zone, SE Spain). *Mar. Pet. Geol.* 2016; **71**: 310-328.
4. Vera JA, Arias C, García-Hernández M, López-Garrido AC, Martín-Algarra S, Martín-Chivelet J, Molina JM, Rivas P, Ruiz-Ortiz PA, Sanz de Galdeano C, Vilas L. Las zonas externas béticas y el paelomargen sudibérico. In: Vera JA, editor. *Geología de España*. Sociedad Geológica de España e Instituto Geológico de España; 2004, p. 354-360.
5. McLennan S. Rare earth elements in sedimentary rocks; influence of provenance and sedimentary processes. *Rev. Mineral. Geochemistry* 1989; **21**: 277-290.
6. Veizer J, Ala D, Azmy K, Bruckschen P, Buhl D, Bruhn F, Carden GAF, Diener A, Ebneth S, Godderis Y, Jasper T, Korte C, Pawellek F, Podlaha OG, Strauss H. $^{87}Sr/^{86}Sr$, $\delta^{13}C$ and $\delta^{18}O$ evolution of Phanerozoic seawater. *Chem. Geol.*1999; **161**: 59-88.
7. Bau M, Balan S, Schmidt K, Koschinsky A. Rare earth elements in mussel shells of the Mytilidae family as tracers for hidden and fossil high-temperature hydrothermal systems. *Earth Planet. Sci. Lett.* 2010; **299**: 310-316.
8. Bau M, Dulski P. Comparing yttrium and rare earths in hydrothermal fluids from the Mid-Atlantic Ridge: Implications for Y and REE behaviour during near-vent mixing and for the Y/Ho ratio of Proterozoic seawater. *Chem. Geol.* 1999; **155**: 77-90.
9. Mazumdar A, Tanaka K, Takahashi T, Kawabe I. Characteristics of rare earth element abundances in shallow marine continental platform carbonates of Late Neoproterozoic successions from India. *Geochem. J.* 2003; **37**: 277-289.
10. Möller P, Dulski P, Bau M. Rare-earth element adsorption in a seawater profile above the East Pacific Rise. *Chemie der Erde - Geochemistry*; 1994; **54**: 129-149.
11. Azmy K, Brand U, Sylvester P, Gleeson SA, Logan A, Bitner MA. Biogenic and abiogenic low-Mg calcite (bLMC and aLMC): Evaluation of seawater-REE composition, water masses and carbonate diagenesis. *Chem. Geol.* 2011; **280**:180-190.

ANEXO

4

Evidencias geoquímicas y simulaciones de transporte de calor para la involucración de fluidos calientes en la formación del depósito de MVT en la zona de Riópar (Cuenca Prebética, SE de España)

Geochemical Evidences and Heat-transport Simulations for Warm Fluid Involvement in the Formation of Riópar MVT Deposit (Prebetic Basin, SE Spain)

Dídac Navarro-Ciurana, Mercè Corbella, Albert Griera, David Gómez-Gras, Esteve Cardellach
Departament de Geologia, Facultat de Ciències, Universitat Autònoma de Barcelona, 08193 Bellaterra (Spain).

Elena Vindel
Departamento de Cristalografía y Mineralogía, Facultad de C. Geológicas, Universidad Complutense de Madrid, 28040 Madrid (Spain).

Linda Daniele
Departamento de Geología, Facultad de C. Físicas y Matemáticas, Universidad de Chile, 13518 Santiago (Chile).

Abstract. The Zn deposits of the historic mines of Riópar (SE Spain) are hosted by dolomitized Cretaceous carbonates bounded by regional scale faults. They constitute a good example of MVT mineralization, where the relations between deposition, heat-transfer and fluid-flow can be easily studied. Geological and geochemical data were used to constrain numerical simulations of fluid mass and heat distribution. The temperatures obtained from Ga/Ge geothermometry in sphalerite (average of 230ºC) are similar to those measured in fluid inclusions from dolomite and sphalerite crystals (T_h mode of 205ºC) and calculated from sphalerite-galena sulfur isotope geothermometry (157±15ºC), suggesting that the fluid temperature did not vary substantially between the source region and the precipitation area. The results of numerical calculations are compatible with advection of fluid and heat through the main faults of the area and along permeable strata. After more than 0.5 Ma of simulation time the temperature distribution in the MVT area range from 140 to 230ºC reflecting the variations observed with sulfur isotope data and fluid inclusion T_h's. Whereas San Jorge fault appears to be the principal conduit to fluid and heat flow, Socovos seems to have acted as a thermal barrier during Late Cretaceous-Early Tertiary times.

Keywords. SE Spain, Riópar MVT ore, Fluid inclusion, Ga/Ge geothermometry, Heat-transport simulation.

1 Introduction

The controls on heat-transport and fluid-flow in Zn-Pb Mississippi Valley-type (MVT) deposits are not well understood. Ore deposition is spatially associated with dolomitized rocks, but the fluid flow regime for hydrothermal dolomitization (one Mg-rich fluid: Gomez-Rivas et al., 2010; Corbella et al., 2014) doesn't seem to match the regime of ore deposition (mixing of hydrothermal fluids: Corbella et al., 2004). Most of the existing MVT deposits case studies reported in the literature have been carried out from stratigraphic, petrographic and geochemical approaches (e.g. Grandia et al., 2003). The final outcome of these contributions is normally a conceptual model illustrated by schematic cartoons. However, improving of the computational and numerical techniques currently allow to integrate field observations, petrographic characterization and geochemical data into fluid and heat flow simulations. These help in visualizing and discriminating between unrealistic hypothesis from those compatible with geological and geochemical data.

The small Riópar ore of the Prebetic basin (SE Spain) provides a clear example of the relationship between Zn-(Pb) deposition, dolomitization and warm fluid and heat flow through fractures. Petrography, Ga/Ge, sulfur isotope and fluid inclusion geothermometry data from the historic Riópar mines were integrated into heat-transport and fluid-flow numerical simulations. The results are presented in this study with the purpose of evaluating temperature distribution and investigating the controls on hydrothermal flow.

2 The Riópar Zn-(Pb) MVT deposit

The Riópar area contains several small and irregular bodies of Zn-(Pb) ore (~20,000 t of extracted Zn metal). They are located at the limit between the External and Internal Prebetic Basins (N boundary of the Mesozoic Betic Rift, SE Spain: Fig. 1). The area is constituted by carbonates and detrital rocks (>2000 m thick: Vera et al., 2004) of Triassic, Jurassic and Cretaceous ages which in turn are covered by Tertiary sediments.

The mineralization is hosted by dolostones replacing a carbonate sequence of Upper Jurassic to Lower Cretaceous age. The Zn-Pb ores are found within the Upper Member of the Puerto Lorente Fm aligned along the footwall block of the W-E-trending and S-dipping San Jorge extensional fault. The Zn-Pb mineralization is distributed in three mining areas: San Agustín, Rosita and San Jorge. The Socovos-San Jorge system fault may have acted as structural control for fluid circulation: such fluid may be responsible for dolomitizing and mineralizing the carbonate units (Navarro-Ciurana et al., 2014).

Zn-Pb MVT deposits in the Maestrat and Basque-Cantabrian Mesozoic basins, in the E and N of the Iberian Peninsula, have been dated as Early to Late Tertiary respectively (Grandia et al., 2003; Symons et al., 2009). As the Mesozoic basin in Riópar is tectonostratigraphically akin to those basins, a similar age for the studied deposits seems reasonable. If this were the case, mineralization could have formed as a consequence of basinal brines circulations related to the rift system developed during the break-up of Pangea.

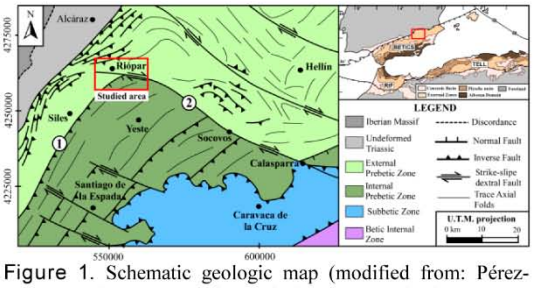

Figure 1. Schematic geologic map (modified from: Pérez-Valera et al., 2010) of the Prebetic Zones and Riópar MVT area. (1) Alto Guadalquivir-San Jorge fault; (2) Socovos fault.

3 Methodology

The mineralogy was studied on thin-polished sections using transmitted and reflected light microscopy at the Dpt. de Geologia of the Universitat Autònoma de Barcelona (UAB). The mineral chemistry was analysed in a JEOL JXA 8900 electron microprobe equipped with a wavelength-dispersive spectrometry (EMPA-WDS) system at the CAI (Universidad Complutense de Madrid). Calibrations were performed using natural and synthetic standards (sphalerite, galena, Fe metal, Cd metal, GaSb, Rb glass). Sulfur isotope analyses were carried out at the Centres Científics i Tecnològics of the Universitat de Barcelona (CCiTUB), using an on-line elemental analyser (EA)-continuous flow-isotope ratio mass spectrometer (IRMS). The S isotope values were reported to the Vienna-Canyon Diablo Triolite (V-CDT) standard. Double-polished 150-µm thick sections were used for the petrographic and microthermometric fluid inclusion study. Measurements were performed on a Linkam THMS-600 heating-freezing stage at the Dpt. de Geologia of the UAB. CODE-BRIGHT (COupled DEformation, BRIne, Gas and Heat Transport) was used to simulate the heat-transport and fluid-flow (Olivella et al., 1994). The program is able to simulate mechanical deformation coupled with multiphase, non-isothermal flow of fluids in geological environments under transient conditions (Corbella et al., 2004).

4 Results and discussion

4.1 Ore mineralogy

The hypogene ore mineralogy is quite simple and is constituted, in order of abundance, by marcasite, sphalerite and galena. Several generations of dolomites have been distinguished as gangue minerals: i) replacive to sucrosic dolomite (ReD-SuD) that constitutes the ore host-rock (Fig. 2a); ii) pre-ore (SaD-I) and post-ore (SaD-II) saddle dolomite-types filling millimetric to centimetric fractures and conforming vein- and breccia-hosted mineralization (Fig. 2a); and iii) porphyrotopic planar dolomite (PoD), which extensively replaces sphalerite. Besides, the hypogene Zn-Pb-Fe ore has been supergenically altered to non-sulfide Zn-Fe-(Pb) minerals.

Large fibrous fans of marcasite blades with regular termination and conforming plumose and radiating cockscomb textures have been observed. It is highly altered to goethite (Fig. 2b). 'Spear-like' crystals range from 0.3 mm up to 1 mm in length. They occur as filling fractures associated with sphalerite and saddle dolomite. Furthermore, it also appears filling pore space of the host-rock (ReD-SuD dolomite). The most common sphalerite-type consists of granular aggregate crystals of subhedral to euhedral forms (100 µm up to 3 mm). They are zoned with dark brown and red to orange colours (Fig. 2c) and are highly altered to smithsonite. Also, discrete sphalerite crystals have been observed disseminated in the host-dolostone (ReD-SuD). Another type of sphalerite is found in a colloform habit conforming veins of 1 to 2 mm in size. Cubo-octahedral galena has been observed in disseminations related to sphalerite and late saddle dolomite (SaD-II). Euhedral to subhedral galena crystal of sizes ranging from 50 µm to 2 mm are encountered commonly altered to cerussite (Fig. 2d).

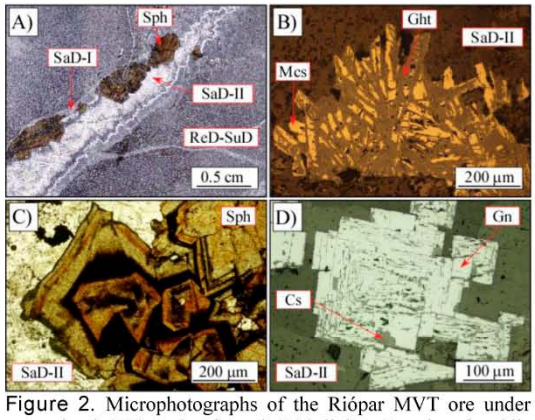

Figure 2. Microphotographs of the Riópar MVT ore under transmitted (TL) and reflected (RL) light: **A)** vein of saddle dolomite related to sphalerite (TL); **B)** plumose marcasite (RL); **C)** aggregate sphalerite (TL); and d) cubo-octahedral galena (RL). ReD-SuD: host-dolostone; SaD-I: early saddle dolomite; SaD-II: late saddle dolomite; Mcs: marcasite; Ght: goethite; Sph: sphalerite; Gn: galena; Cs: cerussite.

4.2 Sphalerite composition, Ga/Ge and sulfur isotope geothermometry

The analyzed major elements of Riópar sphalerite are: 61.26-66.65 wt.% of Zn and 31.76-33.80 wt.% of S (n=92). The range of minor and trace element analyses are: 0.27-4.73 wt.% of Fe (n=92), 0.09-0.71 wt.% of Pb (n=92), 20-5060 ppm of Cd (n=86), 60-2070 ppm of Ga (n=39) and 10-830 ppm of Ge (n=23). Ga/Ge ratio in sphalerite can be used as geothermometer for the ore solution source regions (Möller, 1985). EMPA sphalerite analyses (n=10) show log(Ga/Ge) ratios between -0.09 to 1.59, indicating temperatures from 194 to 252ºC (Fig. 3), with an average of 230ºC.

The sphalerite-galena sulfur isotope geothermometer was used to estimate the formation temperature of the deposit. In only one sample both sulfides were in contact and thus, equilibrium was assumed. The obtained $\delta^{34}S$ values were +1.50‰ and -2.41‰ for sphalerite and galena respectively. From the equation of Ohmoto and Rye (1979) an equilibrium temperature of 157±15ºC was calculated.

4.3 Fluid inclusion geothermometry

Fluid inclusions (FI) can be used to ascertain the minimum temperature of mineral formation (Goldstein and Reynolds, 1994) in the precipitation site. Homogenization temperatures (T_h) were measured on primary FI from different dolomite-types (ReD-SuD, SaD-I, SaD-II) and sphalerite. Most FIs are irregular to elongate in shape with sizes ranging from 3 to 15 µm. T_h values range from 122 to 269ºC. The frequency histogram shows a normal Gaussian distribution, with a mode at 205ºC (n=144) (Fig. 3). Since the sphalerite-galena isotope geothermometre gave a value within the range of the measured T_h's, no pressure correction has been applied. The relatively high T_h's may be explained by advective heat transport with fluids from deeper parts of the Prebetic basin, which may have ascended through the San Jorge-Socovos faults. The wide T_h range observed might be related either to recrystallization phenomena or to fluid temperature variations, either at the deposition site due to mixing or in the source reservoir, or both. The temperature values obtained do not provide clear evidences of fluid mixing, but the presence of a lower temperature fluid component cannot be ruled out and merits further investigations.

The higher values obtained from the Ga/Ge geothermometer (194 to 252ºC) reflect the higher fluid temperatures at the source region with respect to those at the depositional site (122-269ºC). However, the small difference suggests that the hydrothermal fluid temperature did not vary substantially between the source region and the precipitation area, indicating a more or less constant temperature of the ore-bearing fluid during a rapid upflow along the San Jorge Fault.

4.4 Heat-transport and fluid-flow model

Two-dimensional heat and fluid flow simulations were performed in a N-S cross section that, based on our field observations, is representative of the Riópar geology area during Late Cretaceous-Early Tertiary ages (Fig. 5a) The model domain is 9.5 km wide and 3.5 km deep and was discretised using an unstructured triangle mesh refined along and across faults (3320 nodes and 6262 triangles). We assumed that fluid flow was caused by a fluid release through the Socovos-San Jorge sub-vertical system fault connected to the basement rocks, considered to be a possible source for the hydrothermal fluid.

Values for thermal conductivity (1.6-2.7 $W \cdot m^{-1} \cdot K^{-1}$), heat capacity (680-1550 $J \cdot Kg^{-1} \cdot K^{-1}$), and rock density (1970-2800 kg/m^3) of the different units were inferred from data presented by Eppelbaum et al. (2014). The permeabilities and porosities assigned vary from 10^{-17} to 10^{-14} m^2 and 0.15 to 0.3 m^3/m^3 for the different unit rocks, whereas a permeability of 10^{-10} and porosity of 0.8 m^3/m^3 was considered for the active fault zone. The fluid flux at the lower end of the fault was held constant at $1.98 \cdot 10^{-2}$ kg/s and a temperature of 230ºC (estimated from Ga/Ge geothermometer) during the simulation. A temperature gradient of 33 ºC/km and a hydrostatic pressure of 10.1 MPa/km were used as initial conditions (Fig. 5a) and lateral out-flow boundaries were considered for both heat and fluid mass.

The results of the numerical simulations show that a basinal warm fluid would upflow at different Darcy velocities through Socovos and San Jorge faults (on the order of 10^{-10} and 10^{-5} m/s respectively). Thus, heat is mainly funneled with the fluids from San Jorge's fault. Moreover, heat appears to distribute unevenly on the section modeled: high temperature is not only maintained at the fault but also in the Lower Cretaceous sequence of the hanging wall block after 0.5 Ma of simulation time, whereas Triassic rocks basically keep their initial temperature. The model temperature obtained in the precipitation area ranges from 140 to 230ºC, which is consistent with the sphalerite-galena sulfur isotope temperature and T_h's of fluid inclusions in dolomite and sphalerite. According to the parameters of the model, after more than 1 M years of simulation time, heat is predominantly transmitted by advection though the Socovos-San Jorge system fault and the more permeable strata. These faults constitute not only the mechanical N margin of the Internal Prebetic Mesozoic basin, but also its thermal margin, as essentially no heat is escaped from the Socovos fault into the northern strata (Fig. 5b and 5c).

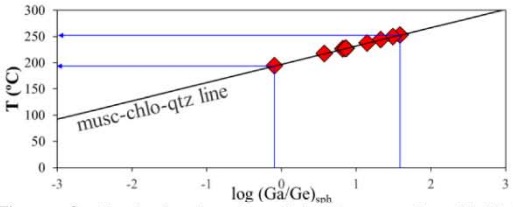

Figure 3. Graph showing the relation between log (Ga/Ge) ratios in sphalerite (diamonds) from Riópar and their formation temperature (arrows). The musc-chlo-qtz line is the chlorite geothermometer in the Si/Al system (Möller, 1985).

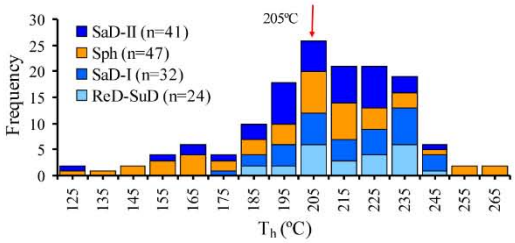

Figure 4. T_h histogram (arrow: T_h mode). ReD-SuD: replacive to sucrosic planar dolomite; SaD-I: early saddle dolomite; Sph: sphalerite; and SaD-II: late saddle dolomite.

5 Conclusions

The ore mineralogy of the Riópar area consists of replacive to sucrosic dolomite, which constitutes the host-rock, an early saddle dolomite followed by marcasite, sphalerite, galena and a late saddle dolomite. Ga/Ge ratios in sphalerite resulted in temperatures from 193 to 253ºC, which reflect the temperature of the fluid reservoir. These temperatures are compatible with sphalerite-galena sulfur isotope temperature (157±15ºC) and T_h measurements on FI in dolomites and sphalerite (122 to 269ºC), that are understood as minimum formation temperature of the MVT deposit.

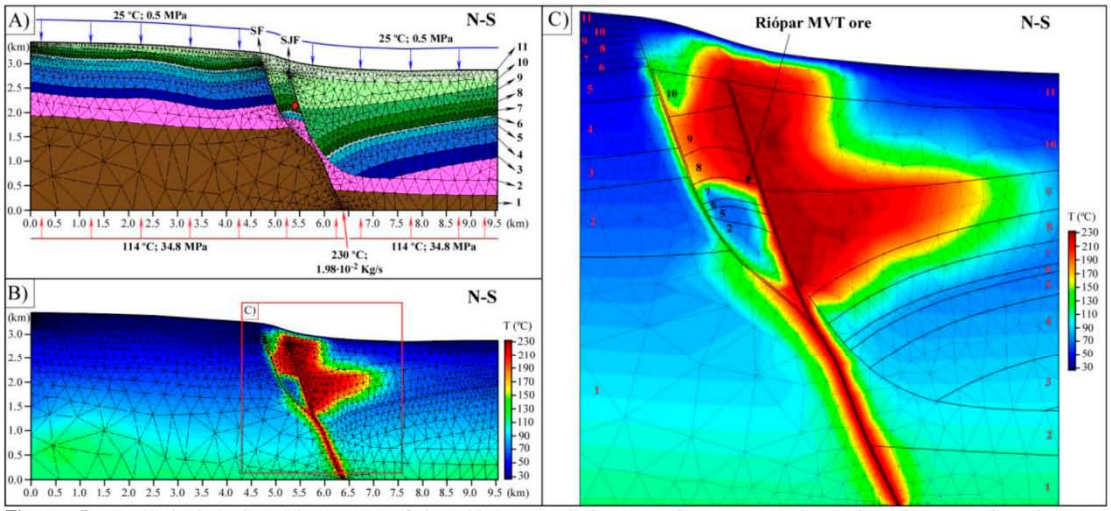

Figure 5. **A)** Geologic units and structure of the Riópar area during Late Cretaceous-Early Tertiary times, mesh and system boundary conditions used in the heat-transport and fluid-flow simulations. Red diamond indicates the localization of the Zn-Pb MVT ores. **B)** and **C)** Simulation results of temperature after 0.8 Ma in a lateral open system. 1) Paleozoic basement (shales and slates); 2) Triassic conglomerates, limestones and clays; 3) Lower Jurassic dolostones; 4) Middle Jurassic dolostones; 5) Upper Jurassic limestones; 6) Upper Jurassic marls; 7) Lower Cretaceous limestones (Upper Mb of the Puerto Lorente Fm); 8) Lower Cretaceous sands (Cerro Lobo Fm) and limestones (Arroyo de los Anchos Fm); 9) Lower Cretaceous sands (Utrillas Fm); 10) Upper Cretaceous limestones (Dolomítica Fm); 11) Upper Cretaceous limestones (Sierra de la Solana Fm); SF: Socovos Fault; SJF: San Jorge Fault.

Integrated field observations and geothermometrical data were used for constraining heat-transport and fluid-flow numerical simulations. The results suggest that mineralizing fluids at Riópar upflowed through the Socovos-San Jorge system fault and invaded and warmed up the host Cretaceous sequence. A temperature of 230ºC in the source region explains the temperatures encountered in the MVT formation area of ~200ºC found after 0.5 Ma of simulation time, remaining stable for more than 1 M years, the time-span when sulfide deposition must have taken place. As suspected by the overlapping temperatures between deposition and source sites, the principal control for heat transfer distribution in the MVT deposits of Riópar is rapid fluid-flow along a fault and permeable strata. According to the simulations presented here, the San Jorge fault acted as the principal conduit to fluid- and heat-flow, whereas the Socovos fault constituted a thermal barrier to the N margin of the Prebetic Mesozoic basin.

Acknowledgements

This research has been supported by the Spanish Ministry of Economy and Competition, through the CGL2011-26488 project. We are grateful to A. Richard for his careful review and constructive criticism of the original manuscript.

References

Corbella M, Ayora C, Cardellach E (2004) Hydrothermal mixing, carbonate dissolution and sulfide precipitation in Mississippi Valley-type seposits. Miner. Deposita 39:344-357

Corbella M, Gomez-Rivas E, Martín-Martín JD, Stafford SL, Teixell A, Griera A, Travé A, Cardellach E, Salas R (2014) Insights to controls on dolomitization by means of reactive transport models applied to the Benicàssim case study (Maestrat Basin, eastern Spain). Pet. Geosci. 20:41-54

Eppelbaum L, Kutsoc I, Pilchin A (2014) Applied Geothermics. Lecture Notes in Earth System Science, pp 1-267

Goldstein TJ, Reynolds RH (1994) Systematics of fluid inclusions in diagenetic minerals. SEPM Short Course 31, pp 1-199

Grandia F, Cardellach E, Canals A, Banks, DA (2003) Geochemistry of the fluids related to epigenetic carbonatehosted Zn-Pb deposits in the Maestrat Basin (Eastern Spain): Fluid inclusion and isotope (Cl, C, O, S, Sr) evidence. Econ. Geol. 98:933-954

Gomez-Rivas E, Corbella M, Martin-Martin JD, Teixell A, Cardellach E (2010) Reactivity of dolomitizing fluids and evaluation of Mg sources in the Benicassim area (Maestrat Basin, E Spain). 72nd EAG Conference and Exhibition 4:2831-2835

Möller P (1985) Development and application of the Ga/Ge-Geothermometer for sphalerite from sediment hosted deposits. In Germann K (ed) Geochemical aspects for Ore Formation in Recent and Fossil Sedimentary Environments. Monograph Series on Mineral Deposits, 25. Geb. Borntraeger, Berlin-Stuttgart, pp 15-30

Navarro-Ciurana D, Vindel E, Cardellach E, Gómez-Gras D, Griera A, Daniele L, Corbella M (2014) Evidence for hot MVT brines in the Mesozoic Prebetic Basin: the Riópar Zn-Pb deposit. Macla (in press)

Ohmoto H, Rye RO (1979) Isotopes sulfur and carbon. In Barnes HL (ed) Geochemistry of Hydrothermal Ore Deposits, second ed. John Wiley and Sons Inc., New York, pp. 509-567

Olivella S, Carrera J, Gens A, Alonso EE (1994) Nonisothermal multiphase flow of brine and gas through saline media. Transport Porous Media 15:271-293

Pérez-Valera LA, Sánchez-Gómez M, Fernández-Soler JM, Pérez-Valera F, Azor A (2010) Diques de lamproítas a lo largo de la Falla de Socovos (Béticas orientales). Geogactea 48:151-154

Symons DTA, Lewchuck M, Kawasaki K, Velasco F, Leach DL (2009): The Rocin zinc-lead deposit, Spain: paleomagnetic dating of a late Tetiary ore body. Miner. Deposita 44:867-880

Vera JA, Arias C, García-Hernández M, López-Garrido AC, Martín-Algarra A, Martín-Chivelet J, Molina JM, Rivas P, Ruiz-Ortiz PA, Sanz de Galdeano C, Vilas L (2004) Las zonas externas béticas y el paleomargen sudibérico. In Vera JA (ed) Geología de España, pp 354-360

UNIVERSITAT AUTÒNOMA DE BARCELONA

DEPARTAMENT DE GEOLOGIA
UNITAT DE CRISTAL·LOGRAFIA I MINERALOGIA

GRUP DE MINERALOGIA APLICADA I
GEOQUÍMICA DE FLUIDS

Memoria presentada por Dídac Navarro Ciurana para optar al grado de Doctor en Geología. La memoria está realizada dentro del Programa de Doctorado en Geología (MEE2011-0492), bajo la dirección de la Dra. M. Mercè Corbella i Cordomí.